NANO LETTERS

2008
Vol. 8, No. 3
897-901

Controllable Formation of Ionic Liquid Micro- and Nanoparticles via a Melt–Emulsion–Quench Approach

Aaron Tesfai,[†] Bilal El-Zahab,[†] David K. Bwambok,[†] Gary A. Baker,[‡] Sayo O. Fakayode,[†] Mark Lowry,[†] and Isiah M. Warner*,[†]

Department of Chemistry, Louisiana State University, Baton Rouge, Louisiana 70803, Chemical Sciences Division, Oak Ridge National Laboratory, Oak Ridge, Tennessee 37831

Received December 5, 2007; Revised Manuscript Received January 17, 2008

ABSTRACT

We present a facile, scalable, and general method for the size-variable generation of monodispersed, near-spherical solid-state (frozen) ionic liquid nanoparticles based on a novel melt−emulsion−quench approach. Simple manipulation of the internal templating droplets within oil-in-water (o/w) microemulsions also permits the formation of well-defined microspheres. This simple and rapid preparation, requiring neither specialized equipment nor harsh conditions, suggests a wealth of potential for these designer nanomaterials within the biomedical, materials, and analytical communities.

Ionic liquids (ILs) are molten salts that generally consist of bulky organic cations paired with charge-diffuse inorganic anions such as PF_6^-, BF_4^-, Tf_2N^-, or NO_3^-.[1–4] The properties of ILs are highly tunable, allowing them to be tailored to meet specific needs by simple variation in either the cation or anion component.[5] In addition, many ILs possess novel properties such as high thermal stability, nonflammability, and essentially zero vapor pressure.[1–6] Because of these unique characteristics, many ILs have been regarded as "green" solvents because their use does not contribute to environmental levels of harmful volatile organic compounds (VOCs), which are traditionally used as industrial solvents.[1,7]

The feasibility of incorporating chiral centers within IL building blocks has recently sparked considerable interest in the use of ILs as chiral solvents and selectors.[8,9] For example, Tran and co-workers have demonstrated that chiral ILs can be used as chiral selectors for diastereomeric interactions in the discrimination of enantiomeric forms of drug molecules.[10] In addition, Ding et al. reported the first use of chiral ILs as novel stationary phases in gas chromatography for the enantiomeric separation of several different compounds.[11]

Apart from their exploration as green solvents and chiral selectors, ILs have also been widely pursued for a range of applications including safer organic reactions (such as the "greening" of Grignard chemistry[12]), analytical chemistry,[3,5] and materials synthesis.[13] For instance, the many benefits attributed to ILs are considered a boon by many researchers in the field of nanotechnology. A number of studies regarding the use of room temperature ILs as polar domains in microemulsions have been published within the past few years.[14–16] A recent review summarizing the use of ILs as media for the synthesis of functional inorganic nanoparticles and other nanostructures has also appeared.[17] In addition, various nanomaterials have been synthesized in IL-based media, including silver, gold, and platinum nanoparticles,[18,19] silver and gold nanowires,[20] and cobalt−platinum nanorods.[21] Furthermore, Kumar et al. recently reported the assembly of conducting organic−metallic composite submicrometer hexagonal rods based on electrostatic complexation between an IL and tetrachloroaurate anions.[22]

Traditionally, the aim has been to produce ILs having melting points well below room temperature to take full advantage of their beneficial solvent properties in reactions, materials synthesis, and separations at near-ambient conditions. In the current literature, only a few published studies have found general utility for ILs with melting points above room temperature (i.e., frozen ILs). For example, Rutten and co-workers demonstrated the use of frozen ILs as substrates for rewritable imaging.[23] However, to our knowledge, the synthesis of a nanoscale material composed of IL species in the frozen state has yet to be reported. We now report the first preparation of uniform and ambient-stable solid (frozen) IL micro- and nanoparticles based on an original oil-in-water

* Corresponding author. E-mail address: iwarner@lsu.edu. Telephone: (225) 578-2829. Fax: (225) 578-3971.
† Department of Chemistry, Louisiana State University.
‡ Chemical Sciences Division, Oak Ridge National Laboratory.

10.1021/nl073184p CCC: $40.75
Published on Web 02/01/2008

Scheme 1. Schematic Showing the Steps Involved in the Melt–Emulsion–Quench Method for Synthesizing Nano- and Microparticles Using Surfactantless (Method 1) and Surfactant-Assisted (Method 2) Procedures[a]

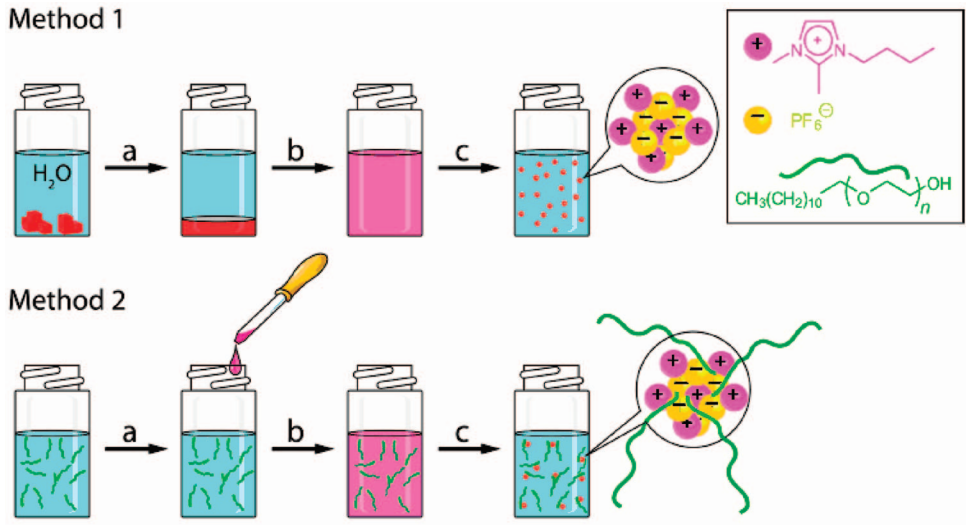

[a] In method 1, the first step (a) entails the melting of [bm_2Im][PF_6] in a hot water bath, whereas dropwise addition of molten [bm_2Im][PF_6] to a surfactant solution is performed at this stage in method 2. The residual steps are homogenization and probe sonication (b), followed by rapid quenching in an ice bath to achieve particle solidification (c).

Scheme 2. Photographs Showing the Various Stages of IL Nanoparticle Formation Following Method 1, as Summarized in Scheme 1[a]

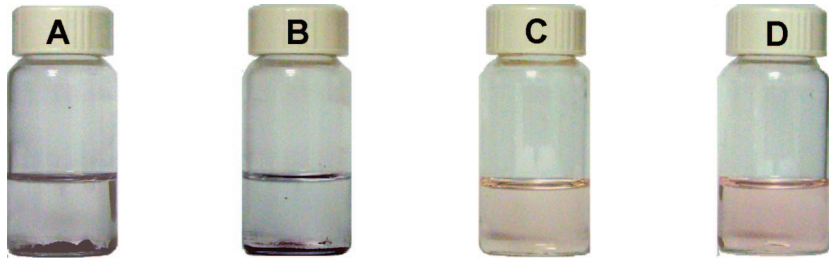

[a] (A) Solid [bm_2Im][PF_6] in water at room temperature; (B) molten-state [bm_2Im][PF_6] phase separated from water at 70°C; (C) o/w emulsion containing [bm_2Im][PF_6] as the inner phase; (D) [bm_2Im][PF_6] nanoparticle crop suspended in water at room temperature. In these images, [bm_2Im][PF_6] was stained with a water-insoluble dye (Nile Red) for visualization purposes.

(o/w) microemulsion approach in which the particle size is correlated to processing conditions.

In this study, we demonstrate proof-of-concept using as a starting material solidified 1-butyl-2,3-dimethylimidazolium hexafluorophosphate ([bm_2Im][PF_6]), an IL with a melting point of 42 °C. IL particles were synthesized using two different procedures, as summarized in Scheme 1. The first method involves the melting and subsequent o/w dispersion of liquid-phase [bm_2Im][PF_6] into water poised well above the IL's melting point, followed by rapid cooling to form discrete solid IL nanoparticles. The second method is conceptually identical; however, in this case, nanoparticles are formed with the aid of an emulsifier, the nonionic surfactant Brij 35. An overview of the melt–emulsion–quench process with photographs illustrating representative stages for method 1 is provided in Scheme 2. It is noteworthy that the lipophilic dye Nile Red used as an aid to visualization does not color the aqueous component of solution but is incorporated into the o/w microemulsion (Scheme 2C) and into the final IL nanoparticles (Scheme 2D). This finding suggests that IL nanoparticles produced in this manner may be used to entrap various materials including drugs and magnetic or sensory agents.

We hypothesize that frozen IL nanoparticles will have distinct properties from traditional nanoparticles in that ILs are broadly tunable, which should reduce the need for chemical activation and/or loading of active ingredients. In fact, we believe that the properties of ILs are sufficiently tunable[4] so as to allow them to mimic the fundamental properties of a vast number of nanoparticle types cited in the current literature.[24–26] We note, for example, a blue-emitting photoluminescent and proton-conductive IL built around a polyamidoamine (PAMAM) dendrimer core[27] and, most recently, phase-tunable fluorophores based upon benzobis(imidazolium) salts.[28] Finally, we believe that frozen ILs, although not intrinsically environmentally friendly or biocompatible, can be designed to possess such properties in addition to their hallmark tunability.

One of the simplest methods to manufacture solid nanoparticles containing active pharmaceutical ingredients (APIs) is through evaporation from emulsion systems, and this topic has been reviewed extensively.[29,30] In this approach, following an emulsification step using high shear mixing with a rotor-stator mixer, high pressure homogenization, or sonication to prepare an o/w or w/o emulsion, particles are formed during solvent evaporation through either increased

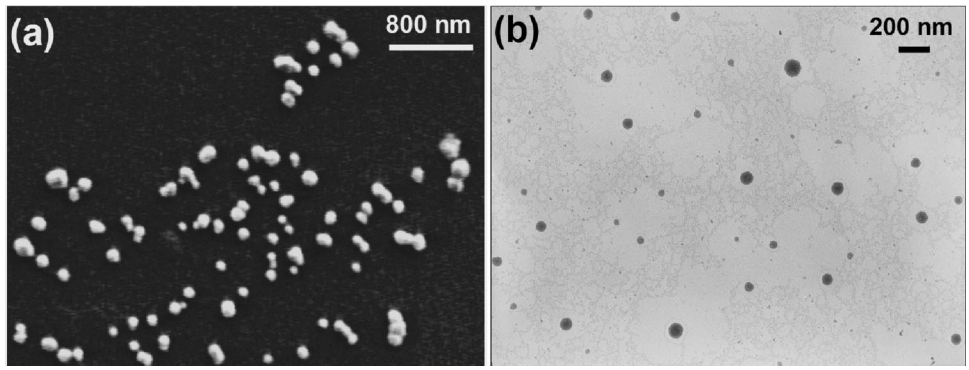

Figure 1. Electron micrographs of [bm_2Im][PF_6] nanoparticles synthesized using method 1: (a) SEM image (15 kV) showing an average nanoparticle diameter of 90 ± 32 nm. (b) TEM image (80 kV) with average nanoparticle diameter measured as 88 ± 34 nm. TEM samples were stained with uranyl acetate.

heat and/or reduced pressure. The melt–emulsion–quench process demonstrated here is well suited to low-melting IL phases and has vastly improved energy efficiency relative to current methods used in API nanoparticle production. This is especially pertinent with regard to the recent emergence of ILs exhibiting antimicrobial activities and bioactivities, most particularly those containing API anions.[31–33]

Using solid, amorphous granules of [bm_2Im][PF_6] as a starting material, the melt–emulsion–quench process in surfactantless mode (method 1) yielded satisfactorily controlled particle sizes having either nanometer or micrometer dimensions, depending on the exact conditions. In a typical preparation, 25 mg of [bm_2Im][PF_6] solid were gently rinsed several times in Ultrapure water (18.2 MΩ cm) and then added to 8 mL of ultrapure water within a 20 mL scintillation vial. The sealed vial was heated at 70 °C in a water bath until the [bm_2Im][PF_6] formed a clear dense liquid phase. The mixture was then homogenized using a commercial homogenizer (PowerGen 125, Fisher Scientific) operating at 30000 rpm for 10 min while the sample was maintained at 70 °C in the water bath. The mixture was then sonicated using a probe ultrasound processor (model CV330, Sonics and Materials Inc., Newton, CT) at 35% intensity for 10 min. Postsonication, the mixture was immediately placed into an ice–water bath to quickly reduce the temperature below the melting point of the IL. The resulting nanoparticles, suspended in the aqueous phase, were washed by use of ultrafiltration (Millipore) three times to remove soluble species. It was found that particle size could be optimized by careful control over experimental conditions: system temperature, homogenization speed and duration, and sonication intensity, duration, and pulse interval sequence.

By following the conditions described above, SEM images show that [bm_2Im][PF_6] nanoparticles with a diameter of 90 ± 32 nm were produced, as shown in Figure 1a, while TEM images of the same sample show that nanoparticles 88 ± 34 nm in diameter were obtained with slightly different morphologies (Figure 1b). It is possible that this difference in morphology results from heat produced from the high-voltage electronic beam, which may have distorted the IL nanoparticles. The nanoparticles were generally spherical and formed a single layer on the TEM grid surface with minimal interparticle aggregation. Aggregation of particles was found to be curtailed by chilling the o/w emulsion on ice, which results in swift IL solidification and so prevents the significant merging of isolated droplets prior to freezing. The average nanoparticle diameter was measured using SEM and TEM imaging and confirmed by dynamic light scattering (DLS). The DLS polydispersity index (PDI), an estimate of the size distribution width, of the as-prepared [bm_2Im][PF_6] nanoparticles was as low as 0.105. Similar procedures can also be used to efficiently generate spherical [bm_2Im][PF_6] particles a few micrometers in diameter. For example, 3 μm microspheres were produced by homogenization of the mixture for 30 s at 30000 rpm then chilled on ice without probe sonication. These microparticles were doped with Nile Red fluorescent dye and imaged using SEM and optical microscopy (Figure 2a–d). The measured dimensions of SEM and optical microscopy images were in agreement, confirming minimal deformation due to the high-voltage electronic beam although slightly better sphericity was observed for the latter.

Emulsifying agents are expected to preferentially orient between the oil (i.e., [bm_2Im][PF_6]) and water phases at the interface of the droplet to prevent coalescence. Consistent with this assumption, the synthesis of nanoparticles using Brij 35 as an emulsifying agent (method 2) yielded more monodispersed nanoparticles. For example, the dropwise addition of 25 mg of [bm_2Im][PF_6], previously melted at 70 °C, to a scintillation vial containing 1.0 wt % Brij 35 in 8 mL of hot ultrapure water during the homogenization period (10 min), followed by treatment similar to that outlined above in method 1, yielded nanoparticles with a diameter of 45 ± 7 nm. Although the nanoparticles from method 2 were generally quite uniform in size, their morphologies appeared more irregular and less spherical than those prepared in the absence of an emulsifying agent (method 1), as can be observed from comparing Figure 1b to Figure 3. The Brij 35 surfactant employed here apparently provides a protective boundary that preserves particle integrity. However, for some applications, a surfactant layer will be undesirable. In other cases, this approach may provide a convenient route for further functionalizing the nanoparticle surface, further expanding the value of IL nanoparticles.

In summary, we have developed a simple, rapid, and high-purity method for efficiently generating tailored frozen IL

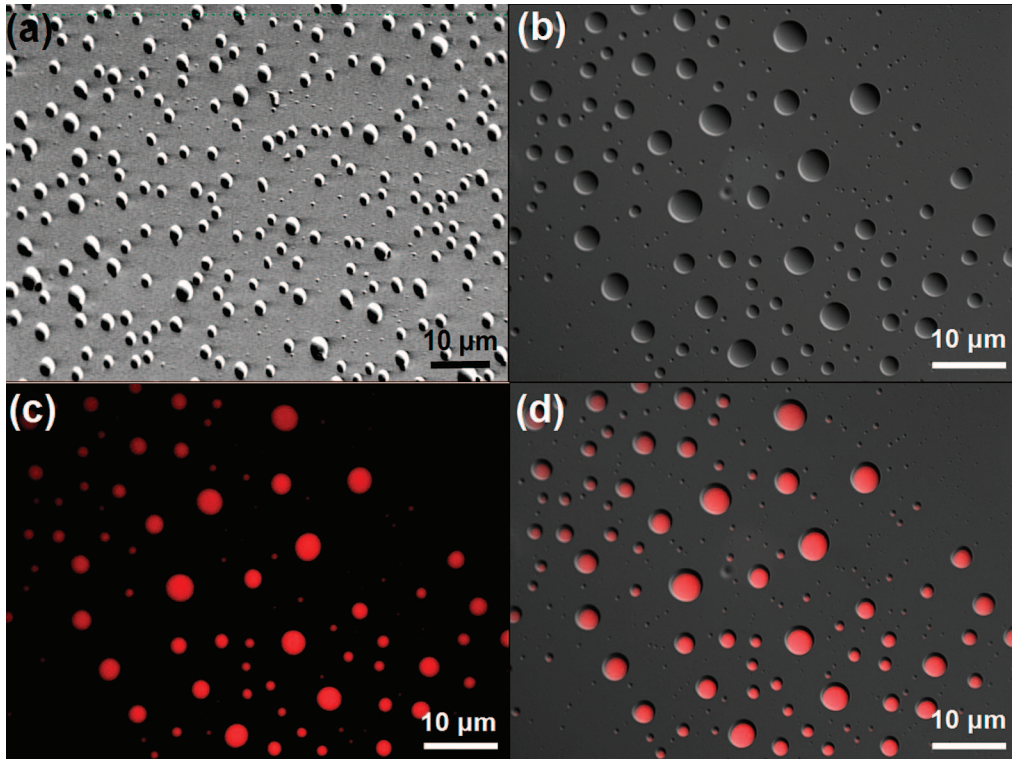

Figure 2. Micrographs of ~3-μm [bm_2Im][PF_6] microparticles prepared following method 1 and imaged using (a) SEM, (b) optical microscopy (DIC), (c) optical microscopy (fluorescence), (d) overlay of DIC and fluorescence images.

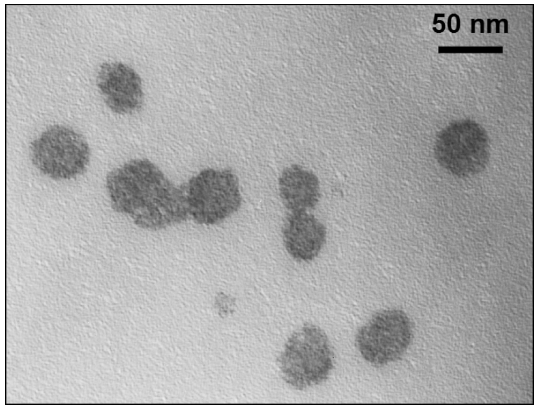

Figure 3. Representative TEM image of 45 ± 7 nm [bm_2Im][PF_6] nanoparticles synthesized based upon method 2, employing Brij 35 as emulsifying agent.

nanoparticles and microspheres under mild conditions based on an original melt–emulsion–quench technique employing the molten IL itself as the oil phase of an o/w microemulsion. No costly or specialized equipment is necessary, and the route requires the addition of organic solvent at no stage of the process. It is expected that particle geometry, dimensions, and composition can be further controlled by varying a number of parameters such as temperature, pressure, surfactant choice, selection of IL building blocks, and emulsion type. For example, creating multiple emulsions such as oil-in-water-in-oil (o/w/o) systems may lead to multiple layers, allowing further flexibility. While the example we provide in this manuscript involves production of a water insoluble nanoparticle, it should be noted that this approach is equally applicable to production of a water soluble nanoparticle. To achieve this, one would simply use a water soluble IL in an organic solvent to carry out the synthesis process using one of the two methods previously outlined. Furthermore, selectively soluble IL for specific applications can be developed for use in certain solvents.

Overall, we believe that nanoparticles synthesized from ILs represent an exciting new direction in nanochemistry. On the basis of our knowledge of IL chemistry, we anticipate that these results will lead to novel utility in a variety of areas including biomedical imaging, displays, intelligent inks, actuators, sensory devices, fuel cells, self-healing materials, and separations.

Acknowledgement. This work was supported by the National Science Foundation, the National Institutes of Health, and the Philip W. West Endowment. The authors thank Gabriela Ganea for assistance with TEM studies and Hadi Marwani for technical assistance.

References

(1) Anderson, J. L.; Ding, R.; Ellern, A.; Armstrong, D. W. *J. Am. Chem. Soc.* **2005**, *127*, 593–604.
(2) Earle, M. J.; Seddon, K. R. *Pure Appl. Chem.* **2000**, *72*, 1391–1398.
(3) Baker, G. A.; Baker, S. N.; Pandey, S.; Bright, F. V. *Analyst* **2005**, *130*, 800–808.
(4) Fei, Z.; Geldbach, T. J.; Zhao, D.; Dyson, P. J. *Chem.—Eur. J.* **2006**, *12*, 2122–2130.
(5) Stalcup, A. M.; Cabovska, B. *J. Liq. Chromatogr. Relat. Technol.* **2004**, *27*, 1443–1459.
(6) Deetlefs, M.; Seddon, K. R.; Shara, M. *Phys. Chem. Chem. Phys.* **2006**, *8*, 642–649.

(7) Huddleston, J. G.; Willauer, H. W.; Swatloski, R. P.; Visser, A. E.; Rogers, R. D. *Chem. Commun.* **1998**, 1765–1766.
(8) Baudequin, C.; Baudoux, J.; Levillain, J.; Cahard, D.; Gaumont, A.-C.; Plaquevent, J.-C. *Tetrahedron: Asymmetry* **2003**, *14*, 3081–3093.
(9) Bwambok, D. K.; Marwani, H. M.; Fernand, V. E.; Fakayode, S. O.; Lowry, M.; Negulescu, I.; Strongin, R. M.; Warner, I. M. *Chirality* **2008**, *20*, 151–158.
(10) Tran, C. D.; Oliveira, D. *Anal. Biochem.* **2006**, *356*, 51–58.
(11) Ding, J.; Welton, T.; Armstrong, D. W. *Anal. Chem.* **2004**, *76*, 6819–6822.
(12) Ramnial, T.; Ino, D. D.; Clyburne, J. A. C. *Chem. Commun.* **2005**, 325–327.
(13) Li, Z.; Liu, Z.; Zhang, J.; Han, B.; Du, J.; Gao, Y.; Jiang, T. *J. Phys. Chem. B* **2005**, *109*, 14445–14448.
(14) Eastoe, J.; Gold, S.; Rogers, S. E.; Paul, A.; Welton, T.; Heenan, R. K.; Grillo, I. *J. Am. Chem. Soc.* **2005**, *127*, 7302–7303.
(15) Gao, H.; Li, J.; Han, B.; Chen, W.; Zhang, J.; Zhang, R.; Yan, D. *Phys. Chem. Chem. Phys.* **2004**, *6*, 2914–2916.
(16) Gao, Y.; Wang, S.; Zheng, L.; Han, S.; Zhang, X.; Lu, D.; Yu, L.; Ji, Y.; Zhang, G. *J. Colloid Interface Sci.* **2006**, *301*, 612–616.
(17) Antonietti, M.; Kuang, D.; Smarsly, B.; Zhou, Y. *Angew. Chem., Int. Ed.* **2004**, *43*, 4988–4992.
(18) Wang, Y.; Yang, H. *Chem. Commun.* **2006**, 2545–2547.
(19) Kim, K.-S.; Demberelnyamba, D.; Lee, H. *Langmuir.* **2004**, *20*, 556–560.
(20) Bhatt, A. I.; Mechler, A.; Martin, L. L.; Bond, A. M. *J. Mater. Chem.* **2007**, *17*, 2241–2250.
(21) Wang, Y.; Yang, H. *J. Am. Chem. Soc.* **2005**, *127*, 5316–5317.
(22) Kumar, A.; Murugesan, S.; Pushparaj, V.; Xie, J.; Soldano, C.; John, G.; Nalamasu, O.; Ajayan, P. M.; Linhardt, R. J. *Small* **2007**, *3*, 429–433.
(23) Rutten, F. J. M.; Tadesse, H.; Licence, P. *Angew. Chem., Int. Ed.* **2007**, *46*, 4163–4165.
(24) Wang, L.; Tan, W. *Nano Lett.* **2006**, *6*, 84–88.
(25) Ding, L.; Olesik, S. V. *Nano Lett.* **2004**, *4*, 2271–2276.
(26) Bruchez, M., Jr.; Moronne, M.; Gin, P.; Weiss, S.; Alivisatos, A. P. *Science* **1998**, *281*, 2013–6.
(27) Huang, J.-F.; Luo, H.; Liang, C.; Sun, I. W.; Baker, G. A.; Dai, S. *J. Am. Chem. Soc.* **2005**, *127*, 12784–12785.
(28) Boydston, A. J.; Pecinovsky, C. S.; Chao, S. T.; Bielawski, C. W. *J. Am. Chem. Soc.* **2007**, *129*, 14550–14551.
(29) Solans, C.; Izquierdo, P.; Nolla, J.; Azemar, N.; Garcia-Celma, M. J. *Curr. Opin. Colloid Interface Sci.* **2005**, *10*, 102–110.
(30) Krauel, K.; Pitaksuteepong, T.; Davies, N. M.; Rades, T. *Am. J. Drug Delivery* **2004**, *2*, 251–259.
(31) Trewyn, B. G.; Whitman, C. M.; Lin, V. S.-Y. *Nano Lett.* **2004**, *4*, 2139–2143.
(32) Laali, K. K., *Ionic Liquids in Synthesis*; Georg Thieme Verlag: Stuttgart, Germany, 2003; Vol. 11, p 1752.
(33) Hough, W. L.; Smiglak, M.; Rodriguez, H.; Swatloski, R. P.; Spear, S. K.; Daly, D. T.; Pernak, J.; Grisel, J. E.; Carliss, R. D.; Soutullo, M. D.; Davis, J. J. H.; Rogers, R. D. *New J. Chem.* **2007**, *31*, 1429–1436.

NL073184P